Dufour and Soret Effects on MHD Flow Near a Stagnation Point

Akin Mike Okedoye
Department of Mathematics, Covenant University, P.M.B. 1023, Ota, Ogun State, Nigeria

Abstract: This study, investigate the effects of Dufour and Soret number on flow of a viscous incompressible electrically conducting fluid in the presence of uniform transverse magnetic field with variable thermal conductivity and non uniform heat source/sink near a stagnation point on a non-conducting stretching sheet. The equations of continuity, momentum and energy are transformed into ordinary differential equations and solved numerically using shooting method together with generalised Thomas algorithm. The velocity, temperature and concentration distributions are discussed numerically and presented through figures. Skin-friction coefficient, the Nusselt and Sherwood number at the sheet are derived, discussed numerically and their numerical values for various values of physical parameter are presented through table.

Key words: Steady, boundary layer, MHD, variable thermal conductivity, stagnation point, heat source/sink, stretching sheet, skin-friction

INTRODUCTION

In fluid dynamics, a stagnation point is a point in a flow field where the local velocity of the fluid is zero. Stagnation points exist at the surface of objects in the flow field where the fluid is brought to rest by the object. A stagnation point occurs whenever a flow impinges on a solid object.

Study of heat transfer in boundary layer over stretching surface find applications in extrusion of plastic sheets, polymer, spinning of fibers, cooling of elastic sheets, etc. The quality of final product depends on the rate of heat transfer and therefore cooling procedure has to be controlled effectively. The MHD flow in electrically conducting fluid can control the rate of cooling and the desired quality of product can be achieved. Liquid metals have small Prandtl number of order $0.01 \sim 0.1$ (e.g., $Pr = 0.01$ is for Bismuth, $Pr = 0.023$ for mercury, etc.) and are generally used as coolants because of very large thermal conductivity. Flow in the neighborhood of a stagnation point in a plane was initiated by Hiemenz. Fluid flow and heat transfer characteristics on stretching sheet with variable temperature condition have been investigated by Grubka and Bobba (1985) (Fig. 1).

Chamkha and Khaled (2000) considered Hiemenz flow in the presence of magnetic field through porous media. Sharma and Mishra (2001) investigated steady MHD flow through horizontal channel: Lower being a stretching sheet and upper being a permeable plate bounded by porous medium. Sriramalu *et al.* (2001) studied steady flow and heat transfer of a viscous incompressible fluid flow through porous medium over a stretching sheet. Mahapatra and Gupta (2001)
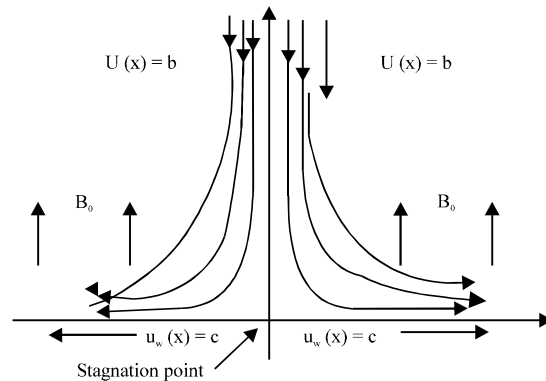

Fig. 1: Physical configuration and coordinate

investigated the magneto hydrodynamic stagnation-point flow towards isothermal stretching sheet and pointed that velocity decreases/increases with the increase in magnetic field intensity when free stream velocity is smaller/greater, repectively than the stretching velocity. Mahapatra and Gupta (2002) studied heat transfer in stagnation-point flow towards stretching sheet with viscous dissipation effect. Khan *et al.* (2003) presented viscoelastic MHD flow, heat and mass transfer over a porous stretching sheet with dissipation energy and stress work. Pop *et al.* (2004) discussed the flow over stretching sheet near a stagnation point taking radiation effect. Seddeek and Salem (2005) investigated the heat and mass transfer distributions on stretching surface with variable viscosity and thermal diffusivity. Recently Okedoye and Bello (2008), discussed MHD flow of a uniformly stretched vertical permeable surface under oscillatory suction velocity and Sharma and Singh (2009) report the

effects of variable thermal conductivity and heat source/sink on MHD flow near a stagnation point on a linearly stretching sheet.

Aim of the present study is to investigate effects of Dufor, Soret numbers, heat and source/sink on flow of a viscous incompressible electrically conducting fluid and heat transfer on a non-conducting stretching sheet in the presence of transverse magnetic field near a stagnation point. Linear stretching of the sheet is considered because of its simplicity in modelling of the flow and heat transfer over stretching surface and further it permits the similarity solution which are useful in understanding the interaction of flow field with temperature field. The heat source/sink is included in the work to understand the effect of internal heat generation and absorption (Sharma and Singh, 2009).

Formulation of the problem: Consider the two dimensional stagnation point flow of a viscous incompressible electrically conducting fluid impinging perpendicular to a permeable plane directed along the x-axis. This is an example of a plane potential flow which arrives from the entire space earliar the plate and impinges on a flat wall placed at y = 0, divides into two streams on the wall and leaves in both directions. Here (u, v) are the components of velocity at any point (x, y) for the viscous flow whereas (U, V) are the velocity components for the potential flow. A uniform magnetic field B_0 is applied normal to the plane.

Then for the two-dimensional steady state flow, the continuity and momentum equations, using the usual boundary layer approximations (Okedoye and Bello, 2008) and by introducing Lorentz force, reduce to:

$$\frac{\partial u}{\partial x} + \frac{\partial v}{\partial y} = 0 \qquad (1)$$

$$u\frac{\partial u}{\partial x} + v\frac{\partial v}{\partial y} = U\frac{dU}{dx} + v\frac{\partial^2 u}{\partial y^2} + \frac{\sigma B_0^2}{\rho}\left(U(x) - u\right) = 0 \quad (2)$$

The boundary conditions for the velocity problem, assuming the absence of magnetic field in the potential flow region are given by:

$$\begin{cases} y = 0 : u(x,0) = cx, v(x,0) = 0 \\ y \to \infty : u(x,\infty) = U(x) = bx \\ \qquad\qquad v(x,\infty) = v(x) = -ax \end{cases} \qquad (3)$$

The temperature distribution can be found from the energy equation which may be written as (neglecting the dissipation):

$$\rho c_p\left(u\frac{\partial T}{\partial x} + v\frac{\partial T}{\partial y}\right) = \frac{\partial}{\partial y}\left(k'\frac{\partial T}{\partial y}\right) + \frac{Dmk_T}{Tm}\frac{\partial^2 C}{\partial y^2} + Q\left(T - T_\infty\right) \qquad (4)$$

Following Arunachalam and Rajappa (1978) and Chaim (1998) the thermal conductivity k' is taken of form as given:

$$k' = k\frac{T}{T_\infty}$$

The boundary conditions for the temperature problem are given by:

$$T(x,0) = T_w, \ T(x,\infty) = T_\infty \qquad (5)$$

Also, the reactant concentration distribution equation can be written as:

$$\rho\left(u\frac{\partial C}{\partial x} + v\frac{\partial C}{\partial y}\right) = Dm\frac{\partial^2 C}{\partial x^2} + \frac{Dmk_T}{Tm}\frac{\partial^2 T}{\partial y^2} - A_0\left(C - C_\infty\right) \qquad (6)$$

Where:
C = The concentration of the chemical species
Dm = Mass diffusion coefficient at constant pressure
A_0 = The chemical reactant parameter of the fluid

The boundary conditions for the reactant problem are given by:

$$C(x,0) = C_w, C(x,\infty) = C_\infty \qquad (7)$$

MATERIALS AND METHODS

Method of solution: By introducing the following dimensionless variables and parameters:

$$\eta = \sqrt{\frac{c}{\upsilon}}y, u(x,y) = cxf'(\eta), v(x,y)$$

$$= -\sqrt{c\upsilon}f(\eta), \theta(\eta) = \frac{T - T_\infty}{(T_w - T_\infty)}, \phi(\eta) = \frac{C - C_\infty}{(C_w - C_\infty)}$$

The governing equations together with the boundary conditions Eq. 1-7 reduced to:

$$f''' + ff'' + M^2\left(\lambda - f'\right) - f'^2 = 0 \qquad (8)$$

$$(1 + \varepsilon\theta)\theta'' + Pr(\varepsilon\theta' + f)\theta' + Pr\beta\theta = -Du\phi'' \qquad (9)$$

$$\phi'' + Sc\left(\phi'f - f\phi\right) = -Sr\theta'' \qquad (10)$$

$$\begin{cases} f(y)=0, f'(y)=1 \\ \theta(y)=1, \phi(y)=1 \quad \text{at} \quad y=0 \\ f'(y)\rightarrow\lambda, \theta(y)\rightarrow 0 \\ \phi(y)\rightarrow 0 \qquad\quad \text{at} \quad y\rightarrow\infty \end{cases} \qquad (11)$$

Here, primes denote differentiation with respect to η. Where:

$$Sc=\frac{\upsilon}{D}, Pr=\frac{\mu c_P}{k}, \beta=\frac{Q}{c\rho c_P}, \alpha=\frac{A_0}{c\rho}$$

$$Du=\frac{Dmk_T}{c_s c_p \upsilon}\left(\frac{C_w-C_\infty}{T_w-T_\infty}\right), Sr=\frac{k_T}{T_m}\left(\frac{T_w-T_\infty}{C_w-C_\infty}\right)$$

The flow Eq. 8-11 subject to boundary conditions (11) are solved numerically using finite differences. A shooting technique is first applied to convert the higher order derivatives to a system of first order differential equations.

The solution for the non-magnetic case is chosen as an initial guess and the iterations using Euler scheme are continued till convergence within prescribed accuracy is achieved with the corrections incorporated in subsequent iterative steps until convergence which is used to obtain the values of the initial guesses. Finally, the resulting guesses together with the system was solved using generalized Thomas' algorithm.

The system of equations has to be solved in the infinite domain $0<\eta<\eta_\infty$. A finite domain in the η-direction can be used instead with η that the solutions are not affected by imposing the asymptotic conditions at a finite distance.

Grid-independence studies show that the computational domain $0<\eta<\eta_\infty$ can be divided into intervals each of uniform step size which = 0.02. This reduces the number of points between $0<\eta<\eta_\infty$ without sacrificing accuracy. The value $\eta_\infty = 10$ was found to be adequate for all the ranges of parameters studied here.

Skin friction, rate of heat and mass transfer
Skin-Friction: Researchers now study skin-friction from velocity field. It is given by:

$$c_f=\frac{T_f}{\rho u_\omega v_\omega}=\frac{d^2}{dy^2}u(y,t)\Big|_{y=0}, \tau f=\mu\frac{du}{dy}\Big|_{y=0}$$

Which reduces to:

$$c_f=\left(\frac{\partial u}{\partial\eta}\right)_{\eta=0}$$

Therefore:

$$c_f=\left(\frac{df(\eta)}{d\eta}\right)_{\eta=0}$$

Nusselt number: In non-dimensional form, the rate of heat transfer at the wall is computed from Fourier's law and is given by:

$$Nu=\frac{q_\omega v}{(T_\omega-T_\infty)Kv_\omega}=\frac{-d}{dy}\theta(y,t)\Big|_{y=0}, q_\omega=-K\frac{dT}{dy}\Big|_{y=0}$$

Therefore:

$$Nu=\frac{d\theta(\eta)}{(d\eta)}\Big|_{\eta=0}$$

Sherwood number: The rate of mass transfer at the wall which is the ratio of length scale to the diffusive boundary layer thickness is given by:

$$Sh=\frac{J_\omega v}{(c_\omega-c_\infty)Dv_\omega}=\frac{d}{dy}\phi(y,t)\Big|_{y=0}, J_\omega=-D\frac{d\phi}{dy}\Big|_{y=0}$$

Which implies:

$$Sh=\frac{d\phi(\eta)}{d\eta}\Big|_{\eta=0}$$

The momentum Eq. 7 has analytical solution when $M = 0$. Researchers compare this results with the numerical result for $M = 0.5$ and 0.8. It is observed from Table 1 that the numerical and analytical values of velocity f' (η) are in good agreement as shown in Table 1. The comparison is satisfactory and this happens for other Pr numbers. In contrast to the earliar numerical solution presented, here the Prandtl number used is one corresponding to the one for plasma (Pr = 0.71).

Table 1: Comparision of analytical and numerical solution for M = 0.5 and 0.8

y	M = 0.5			M = 0.8		
	Analytical	Numerical	Difference	Analytical	Numerical	Difference
0	1.000000	1.000000	0	1.000000	1.000000	0
1	0.326922	0.326921	0.000001	0.277864	0.277864	0
2	0.106878	0.106877	0.000001	0.077208	0.077208	0
3	0.034941	0.034938	0.000003	0.021453	0.021453	0
4	0.011423	0.011420	0.000003	0.005961	0.005961	0
5	0.003734	0.003730	0.000004	0.001656	0.001656	0

Table 1: Continue

y	M = 0.5			M = 0.8		
	Analytical	Numerical	Difference	Analytical	Numerical	Difference
6	0.001221	0.001215	0.000006	0.000460	0.000460	0
7	0.000399	0.000392	0.000007	0.000128	0.000127	0
8	0.000130	0.000122	0.000008	0.000036	0.000035	0.000001
9	0.000043	0.000032	0.000011	0.000010	0.000008	0.000002
10	0.000014	0.000000	0.000014	0.000003	0.000000	0.000003

Special cases: In the absence of magnetic field, i.e., M = 0 the results of the present paper are reduced to those obtained by Pop *et al.* (2004) and Mahapatra and Gupta (2002). In the absence of magnetic field, heat source/sink and variable thermal conductivity, the results of the present study are reduced to those obtained by Pop *et al.* (2004) in the absence of radiation effect with constant thermal conductivity and Mahapatra and Gupta (2002) in absence of viscous dissipation and constant thermal conductivity. In the absence of chemical reaction, the result of the present study are reduced to those obtained by Sharma and Singh (2009).

RESULTS AND DISCUSSION

Velocity, temperature and concentration distributions: Figure 2 and 3 present the velocity profile f' (η) and concentration profile ϕ (η), respectively for various values of λ. Figure 2 and 3 show that increasing the parameter λ increases f' (η) and reduces ϕ (η). However from Fig. 3, it could be deduce that increasing λ reduces concentration boundary layer at a point in the flow field reverse flow occurs which is indicated by the portion of the curve in the negative vertical axis.

Figure 4 presents the temperature profile θ (η) for various values of λ. Figure 4 indicates that the temperature boundary layer thickness decreases as λ increases. It is also clear from Fig. 4 that increasing the ratio of stream velocity to stretching sheet parameter decrease the velocity throughout the boundary layer.

Figure 5 is a graphical representation which depicts the effect of magnetic field parameter M on the velocity profile f_η (η). It is found that the effect of magnetic field parameter M is to reduce the velocity, significantly in the viscous flow; this is due to the fact that increase of M signifies the increase of Lorentz force which opposes the flow in the reverse direction. Increasing M decreases the velocity boundary layer.

Figure 6 and 7 shows the concentration ϕ (η) and temperature θ (η) profiles for various values of M. On comparison of the curves, it is seen that concentration
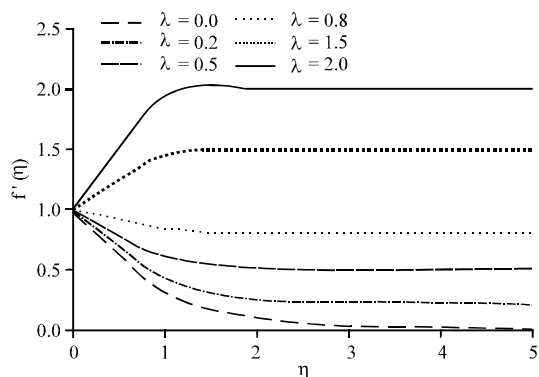

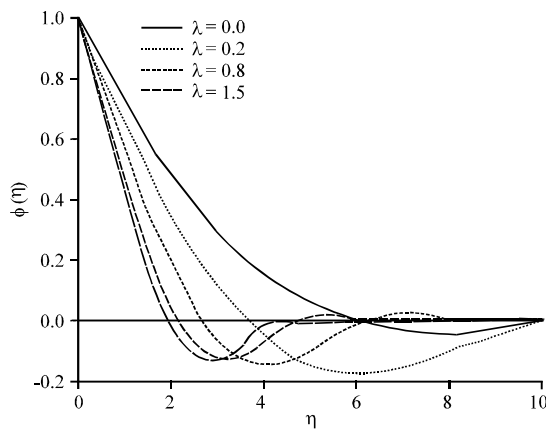Fig. 2: Variation of f, (η) for various values of λ

Fig. 3: Variation of ϕ (η) for various values of λ

increases in the flow region due to the application of magnetic field. Here, increase of magnetic force causes increase of concentration boundary layer thickness in the fluid flow (Fig. 6).

While, the temperature field reduces with an increase in M for $0 < \eta < 4$ beyond which it increases with an increase in M.

The effect of chemical reaction parameter on concentration profile ϕ (η) is shown in Fig. 8. Researchers note that during destructive chemical reaction ($\alpha < 0$) increase in chemical reaction parameter decrease the concentration boundary layer, however the situation is reversed during the occurrence of reverse flow (ϕ (η)<0).
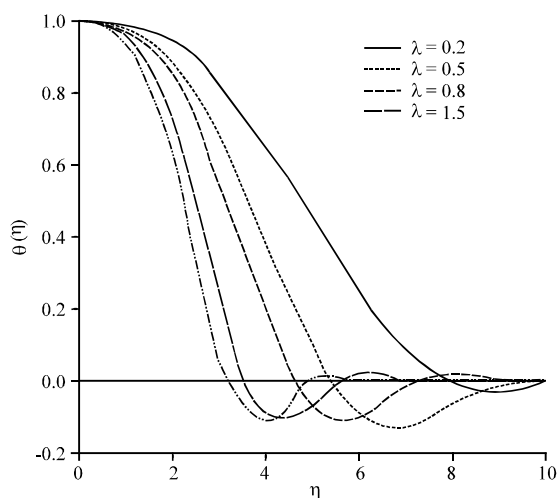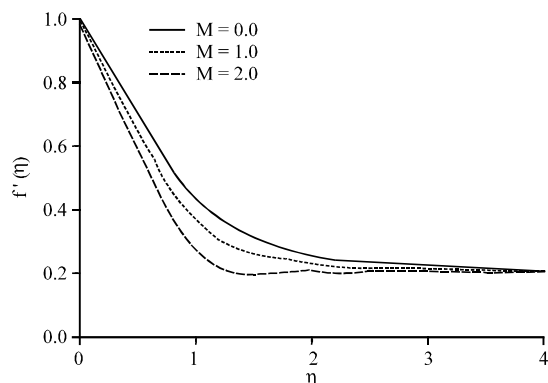
Fig. 4: Variation of θ (η) for various values of λ
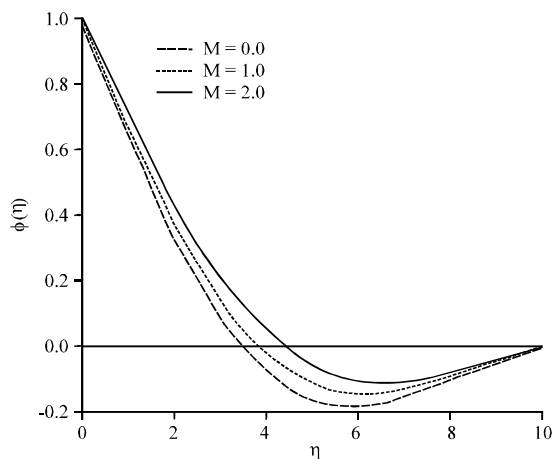

Fig. 5: Variation of f' (η) for various values of M

Fig. 6: Variation of φ (η) for various values of M

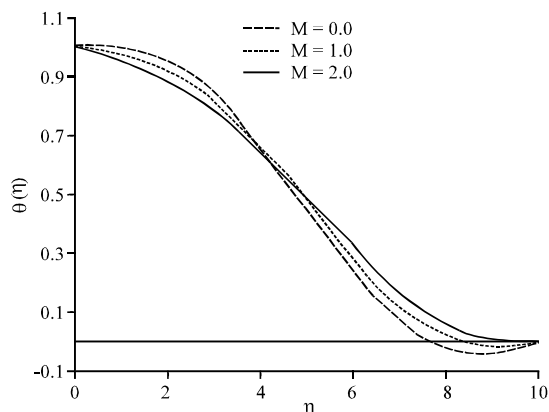In Fig. 9, it is clear that the effect of the α on the thermal boundary layer thickness is significant. Increasing α
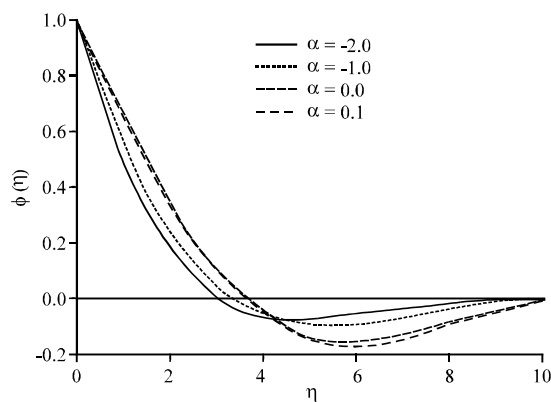

Fig. 7: Variation of θ (η) for various values of M
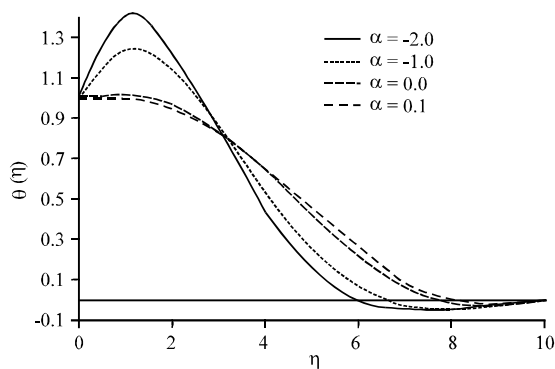

Fig. 8: Variation of φ (η) for various values of α

Fig. 9: Variation of θ (η) for various values of λ

decreases the thermal boundary layer thickness, also researchers not that for destructive chemical reaction, the maximum temperature is not on the surface but in the body of the fluid, this is indicated by the presence of peak in the curves. Far away from the wall (η>3), the temperature distribution is reversed and hence increasing α increases thermal boundary layer.

Figure 10 and 11 shows variation of heat generation/absorption with concentration and temperature distributions, respectively. It could be seen that the fluid concentration reduces as heat generation increases. Furthermore, the maximum concentration is the concentration at the wall for this combination of control parameters. While in Fig. 11, the thermal boundary layer increase wit increase in heat generation, also the presence of peaks in the curves signifies that maximum temperature occur in the body of the fluid.

The effect of Dufour number on the concentration and temperature fields is shown in Fig. 12 and 13, respectively. Researchers observe that Dufour number increases both concentration and temperature distributions. The same thing is observed with Soret number as shown in Fig. 14 and 15. But here, concentration distribution decreases with an increase in Soret number whereas thermal boundary layer increases with increase in Soret number. Figure 16 and 17 is plotted for the concentration and temperature distribution, respectively for various Prandtl number, it is an interesting note that there is a significant enhancement in both cases.

On comparison of the curves, it could be seen that there would be an increase in both concentration and temperature in the flow region for lower values of Prandtl number which result in increase of concentration and thermal boundary layer thickness as Prandtl number decreases. In general for the case here, $Pr<1$ which means
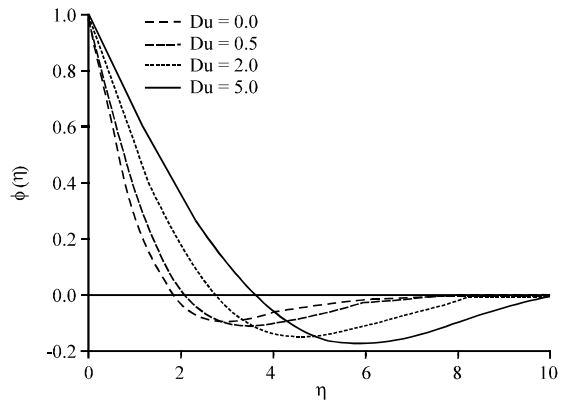

Fig. 12: Variation of ϕ (η) for various values of Du

Fig. 13: Variation of θ (η) for various values of Du

Fig. 10: Variation of ϕ (η) for various values of β

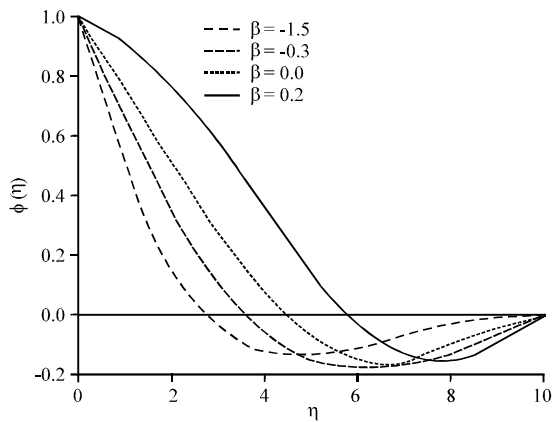Fig. 11: Variation of θ (η) for various values of β

Fig. 14: Variation of ϕ (η) for various values of Sr

Fig. 15: Variation of θ (η) for various values of Sr

Fig. 16: Variation of ϕ (η) for various values of Pr
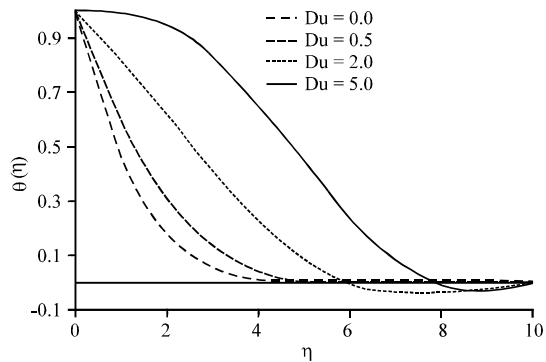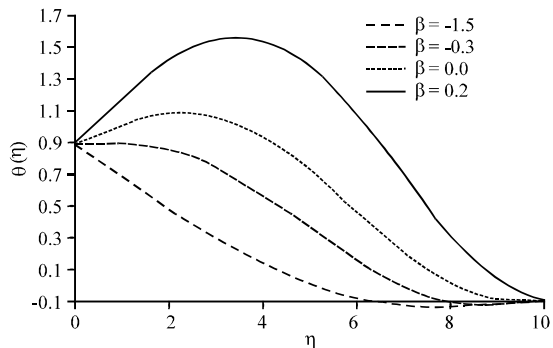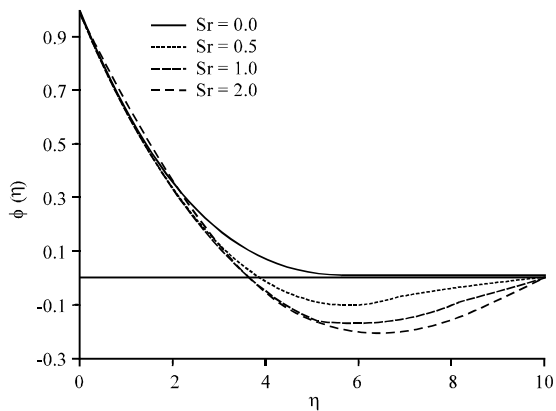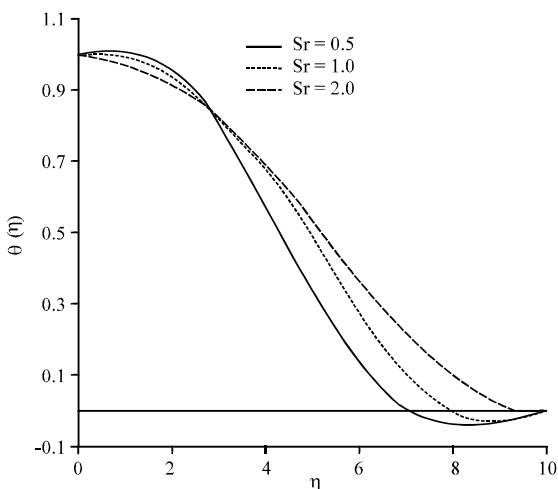

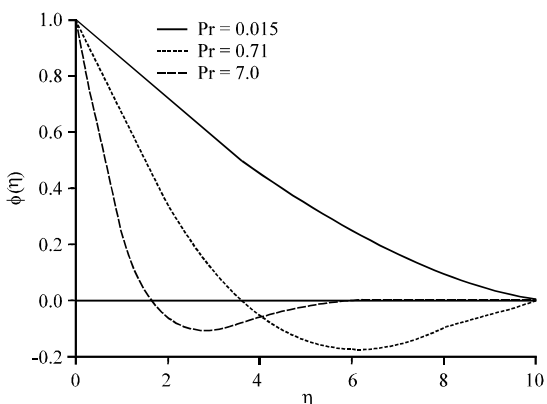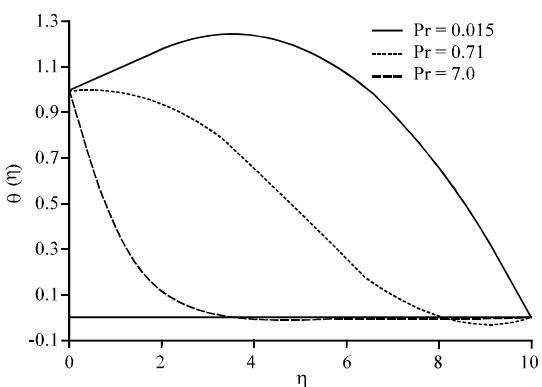Fig. 17: Variation of θ (η) for various values of Pr

Fig. 18: Variation of ϕ (η) for various values of Sc

Fig. 19: Variation of θ (η) for various values of Sc

distribution decreases as the density of the species, thus Ammonia is expected to have the highest concentration distribution followed by water vapour and then hydrogen as depicted in Fig. 18. While temperature distribution increases as Schmidt number increases.

Skin-friction, rate of mass transfer and heat flux: The non-dimensional skin friction (c_f), rate of mass transfer in terms of Sherwood number (Sh) and the heat flux in terms of Nusselt number (Nu) are entered in Table 2 for different values of Hartmann number (M) reaction parameter (α) heat source/sink parameter (β) Dufour number (Du) Soret number (Sr) Prandtl number (Pr) and Schmidt number (Sc).

The effect of this parameters on the non-dimensional skin friction (c_f) rate of mass transfer in terms of Sherwood number (Sh) and the heat flux in terms of Nusselt number (Nu) as shown in Table 2 and 3 is self-evident.

the conduction effects exceeds viscous diffusion the thermal boundary layer is thicker than the velocity boundary layer.

The effect of presence of foreign chemical species is shown in Fig. 18 and 19, it is shown that concentration
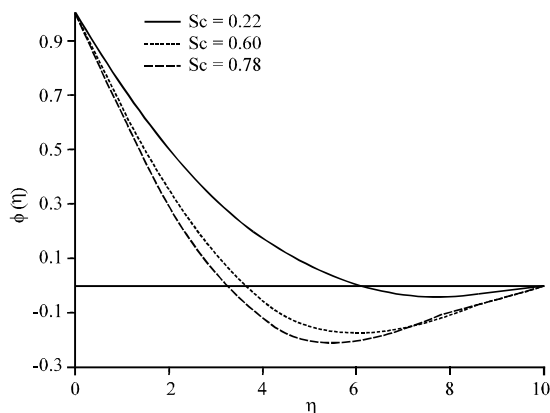
69

Table 2: Effect of various parameters on f' (0), θ' (0) and φ' (0)

λ	M	α	β	Dτ	Sr	Pr	Sc	f'' (0)	θ' (0)	φ' (0)
0.0	0.5	0.1	-0.3	5	1	0.71	0.6	-1.118000	-2.70E-2	-0.370486
0.2	0.5	0.1	-0.3	5	1	0.71	0.6	-1.000470	-0.299578	-0.101500
0.5	0.5	0.1	-0.3	5	1	0.71	0.6	-0.711900	-0.419309	-3.38E-2
0.8	0.5	0.1	-0.3	5	1	0.71	0.6	-0.315410	-0.464700	-2.31E-2
1.5	0.5	0.1	-0.3	5	1	0.71	0.6	0.942791	-0.559220	-1.12E-2
2.0	0.5	0.1	-0.3	5	1	0.71	0.6	2.077725	-0.617970	-4.87E-3
0.2	0.0	0.1	-0.3	5	1	0.71	0.6	-0.918110	-1.86E-2	-0.377000
0.2	0.5	0.1	-0.3	5	1	0.71	0.6	-1.000470	-2.70E-2	-0.370486
0.2	1.0	0.1	-0.3	5	1	0.71	0.6	-1.215620	-4.66E-2	-0.356060
0.2	2.0	0.1	-0.3	5	1	0.71	0.6	-1.842370	-8.61E-2	-0.329000

Table 3: Effect of various parameters on θ' (0) and φ' (0)

α	β	Dτ	Sr	Pr	Sc	θ' (0)	φ' (0)
-2.0	-0.3	5.0	1.0	0.710	0.60	0.844618	-0.600410
-1.0	-0.3	5.0	1.0	0.710	0.60	0.471631	-0.504030
0.0	-0.3	5.0	1.0	0.710	0.60	2.13E-2	-0.383040
0.1	-0.3	5.0	1.0	0.710	0.60	-2.70E-2	-0.370486
0.4	-0.3	5.0	1.0	0.710	0.60	-1.40E-2	-0.414030
0.1	-1.5	5.0	1.0	0.710	0.60	-0.307420	-0.597290
0.1	-0.3	5.0	1.0	0.710	0.60	-2.70E-2	-0.370486
0.1	0.0	5.0	1.0	0.710	0.60	0.111672	-0.245080
0.1	0.2	5.0	1.0	0.710	0.60	0.275211	-7.09E-2
0.1	0.4	5.0	1.0	0.710	0.60	0.785117	0.609847
0.1	-0.3	0.0	1.0	0.710	0.60	-0.678110	-0.897250
0.1	-0.3	0.5	1.0	0.710	0.60	-0.484990	-0.730300
0.1	-0.3	2.0	1.0	0.710	0.60	-0.224080	-0.519750
0.1	-0.3	5.0	1.0	0.710	0.60	-2.70E-2	-0.370486
0.1	-0.3	5.0	0.0	0.710	0.60	6.15E-3	-0.373200
0.1	-0.3	5.0	0.5	0.710	0.60	-2.09E-2	-0.370110
0.1	-0.3	5.0	1.0	0.710	0.60	-2.70E-2	-0.370486
0.1	-0.3	5.0	2.0	0.710	0.60	-4.71E-2	-0.359770
0.1	-0.3	5.0	1.0	0.015	0.60	7.52E-2	-0.141340
0.1	-0.3	5.0	1.0	0.710	0.60	-2.70E-2	-0.370486
0.1	-0.3	5.0	1.0	7.000	0.60	-0.789900	-0.997490
0.1	-0.3	5.0	1.0	0.710	0.22	-0.185180	-0.292240
0.1	-0.3	5.0	1.0	0.710	0.60	-2.70E-2	-0.370486
0.1	-0.3	5.0	1.0	0.710	0.78	0.044913	-0.402350

CONCLUSION

From the earliar discussions, researchers can draw the following conclusion:

- Fluid velocity decreases due to increase in the Hartmann number
- Fluid temperature increases due to increase in the thermal conductivity parameter, the Hartmann number or volumetric rate of heat source parameter
- Rate of heat transfer at the sheet increases due to increase in the Prandtl number or λ while it decreases due to increase in the Hartmann number
- The velocity boundary layer increases as viscousity parameter increases
- Axial velocity decreases with the increase of viscosity parameter
- The fluid temperature reduces as heat generation increases

NOMENCLATURE

k*	=	Variable thermal conductivity
K	=	Uniform thermal conductivity
u, v	=	Velocity components along x- and y-axis, respectively
C	=	Concentration of the fluid
Dm	=	Diffusion coefficient
T	=	Fluid temperature
v	=	Fluid transverse velocity
U	=	Free stream velocity
C_∞	=	Free stream concentration
T_∞	=	Free stream temperature
M	=	Hartmann number
Q	=	Heat generation coefficient
c_p	=	Specific heat at constant pressure
c_w	=	Surface concentration
T_w	=	Surface temperature

Dimensionless group:

Grc	=	Mass Grashof number
Grt	=	Thermal Grashof number
Pr	=	Prandtl number
Sc	=	Schmidt number

Greek letters:

θ	=	Non-dimensional fluid temperature
λ	=	Ratio of free stream velocity parameter to stretching sheet parameter
β	=	Heat source/sink coefficient

β_c =   Coefficient of concentration expansion
β_t =   Coefficient of thermal expansion
Subscripts:
w   =   Condition on the wall
∞ =   Ambient condition

REFERENCES

Arunachalam, M. and N.R. Rajappa, 1978. Forced convection in liquid metals with variable thermal conductivity and capacity. Acta Mechanica, 31: 25-31.

Chaim, T.C., 1998. Heat transfer in a fluid with variable thermal conductivity over a linearly stretching sheet. Acta Mechanica, 129: 63-72.

Chamkha, A.J. and A.R.A. Khaled, 2000. Similarity solutions for hydromagnetic mixed convection heat and mass transfer for Hiemenz flow through porous media. Int. J. Numer. Methods Heat Fluid Flow, 10: 94-115.

Grubka, L.J. and K.M. Bobba, 1985. Heat transfer characteristics of a continuous, stretching surface with variable temperature. J. Heat Transfer, 107: 248-250.

Khan, S.K., A.M. Subhas and R.M. Sonth, 2003. Visco-elastic MHD flow, heat and mass transfer over a porous stretching sheet with dissipation of energy and stress work. Heat Mass Transfer, 40: 47-57.

Mahapatra, T.R. and A.S. Gupta, 2001. Magnetohydrodynamic stagnation-point flow towards a stretching sheet. Acta Mech., 152: 191-196.

Mahapatra, T.R. and A.S. Gupta, 2002. Heat transfer in stagnation-point flow towards a stretching sheet. Heat Mass Transfer, 38: 517-521.

Okedoye, A.M. and O.A. Bello, 2008. MHD flow of a uniformly stretched vertical permeable surface under oscillatory suction velocity. J. Niger. Assoc. Math. Phys., 13: 211-220.

Pop, S.R., T. Grosan and I. Pop, 2004. Radiation effect on the flow near the stagnation point of a stretching sheet. Technische Mechanik, 25: 100-106.

Seddeek, M.A. and A.M. Salem, 2005. Laminar mixed convection adjacent to vertical continuously stretching sheets with variable viscosity and variable thermal diffusivity. Heat Mass Transfer, 41: 1048-1055.

Sharma, P.R. and U. Mishra, 2001. Steady MHD flow through horizontal channel: Lower being a stretching sheet and upper being a permeable plate bounded by porous medium. Bull. Pure Applied Sci., 20E: 175-181.

Sharma, P.R. and G. Singh, 2009. Effects of variable thermal conductivity and heat source/sink on MHD flow near a stagnation point on a linearly stretching sheet. J. Applied Fluid Mech., 2: 13-21.

Sriramalu, A., N. Kishan and R.J. Anand, 2001. Steady flow and heat transfer of a viscous incompressible fluid flow through porous medium over a stretching sheet. J. Energy Heat and Mass Transfer, 23: 483-495.